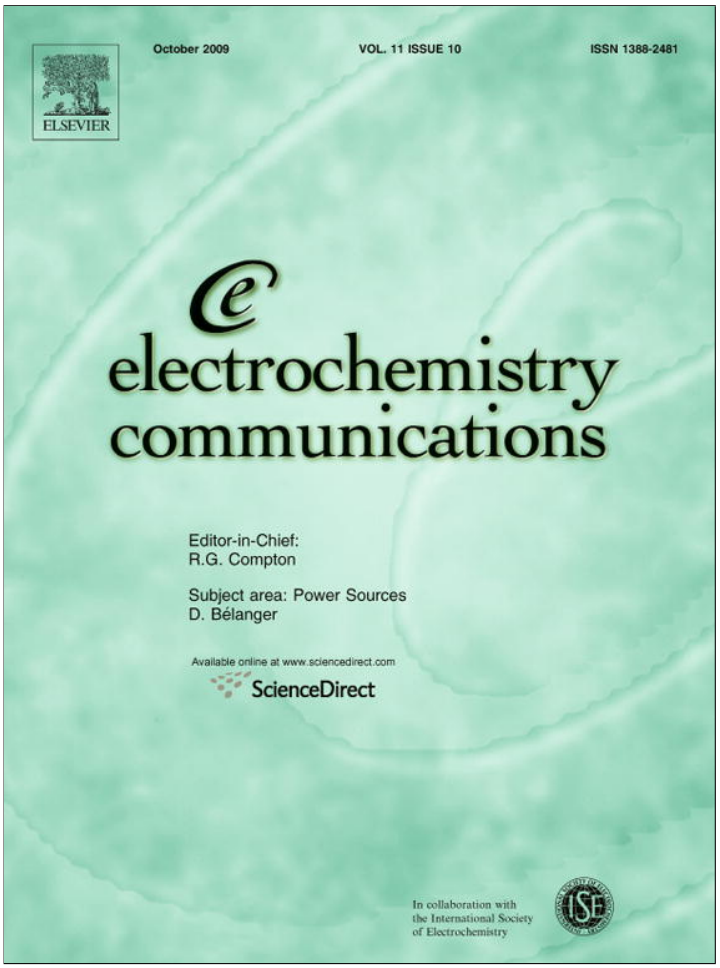

Electrochemistry Communications 11 (2009) 2036–2039

Contents lists available at ScienceDirect

Electrochemistry Communications

journal homepage: www.elsevier.com/locate/elecom

Electrocatalysis on gold nanostructures: Is the {1 1 0} facet more active than the {1 1 1} facet?

Ying Chen [a], Wolfgang Schuhmann [b], Achim Walter Hassel [a,c,*]

[a] Max-Planck-Institut für Eisenforschung GmbH, Max-Planck Str. 1, D-40237 Düsseldorf, Germany
[b] Analytische Chemie – Elektroanalytik & Sensorik, Ruhr-Universität Bochum, Universitätsstr. 150, D-44780 Bochum, Germany
[c] Institute for Chemical Technology of Inorganic Materials, Johannes Kepler University, Altenbergerstr. 69, A-4040 Linz, Austria

ARTICLE INFO

Article history:
Received 22 July 2009
Received in revised form 25 August 2009
Accepted 25 August 2009
Available online 29 August 2009

Keywords:
Anisotropic
Nanobelts
Nanoplates
Glucose
Methanol

ABSTRACT

The anisotropic electrocatalytic properties of gold nanobelts and nanoplates enclosed by either {1 1 0} or {1 1 1} facets were studied. Different strategies were used to synthesize these materials. It was found that the {1 1 0} surface of gold does not necessarily show a higher electrocatalytic activity than the {1 1 1} surface. The {1 1 0} surface of gold is more active than the {1 1 1} surface for glucose oxidation in both, neutral and alkaline media. However, for methanol oxidation in alkaline solution, the {1 1 0} surface shows a lower activity than the {1 1 1} surface, which is contrary to the general belief that {1 1 0} facet is the most active surface among the three basal planes. The possible mechanisms are discussed.

1. Introduction

The electrocatalytic properties of metal nanocrystals highly depend on the exposed surfaces. Experimental results as well as theoretical considerations have emphasized the importance of the anisotropic properties of crystallographic planes [1,2]. Fundamental studies of single crystal planes of noble metals, such as Au, Pd and Pt, demonstrated that the high-index planes possess a higher density of low coordination number step atoms in comparison with low-index planes such as {1 1 1}, {1 0 0}, and even {1 1 0} facets, and exhibit high activity for breaking chemical bonds [2–6]. Thus, shape-controlled synthesis of metal nanocrystals bounded by high-index facets is deemed as a potential route for enhancing their catalytic properties [1,2,5–12]. Recently, Tian et al. reported that tetrahexahedral Pt nanoparticles bounded by {7 3 0}, {2 1 0} and/or {5 2 0} surfaces display an extraordinarily high catalytic activity [1]. Moreover, Liao et al. showed that Au star- and thorn-shaped nanoparticles enclosed by {3 3 1} and vicinal high-index facets show a higher electrocatalytic activity for H_2O_2 reduction [5].

According to the fact that surface energies of different basal planes of fcc metals are in the order of $\gamma_{\{1\,1\,1\}} < \gamma_{\{1\,0\,0\}} < \gamma_{\{1\,1\,0\}}$ [13], it is reasonable to assume that {1 1 0} surface should show the highest electrocatalytic abilities among the three low-index planes. The reports of the structurally and morphologically dependent electrocatalytic properties of nanocrystals are vast [1,2,5–14]. However, in most cases, nanocrystals with different exposed surfaces have different shapes. This is because, generally, the final shape of nanocrystals is determined by exposed surfaces considering the nature of the synthesis method [1,2,5–14]. Gold is known to form preferentially {1 1 1} surface with its low surface energy when being evaporated or sputtered onto a surface or when a bulk material is annealed [15]. Recently, a novel approach was established to prepare Au nanobelts and nanoplates enclosed by {1 1 0} surface, which is less common for gold [16–19]. These unique Au nanostructures, complemented with the traditional wet chemical method, enable to study the differences in properties of nanocrystals with similar shape but different crystallographic termination. In this communication, gold nanobelts with {1 1 0} surface ({1 1 0} nanobelts) and nanoplates with either {1 1 0} or {1 1 1} surface ({1 1 0} nanoplates, {1 1 1} nanoplates) were used to study the anisotropic electrocatalytic properties by employing the electrooxidation of methanol and glucose as probe reactions.

2. Experimental

Gold nanobelts and square-shaped nanoplates with {1 1 0} facets were prepared through the combination of directional decomposition of the Fe–Au eutectoid alloy followed by a phase selective

* Corresponding author. Address: Institute for Chemical Technology of Inorganic Materials, Johannes Kepler University, Altenbergerstr. 69, A-4040 Linz, Austria. Tel.: +49 211 6792; fax: +43 732 2468 8905.
E-mail address: hassel@elchem.de (A.W. Hassel).

1388-2481/$ - see front matter © 2009 Elsevier B.V. All rights reserved.
doi:10.1016/j.elecom.2009.08.046

etching. The hexagonal gold nanoplates with {1 1 1} surface were synthesized by a wet chemical method. The details were described elsewhere [15–20].

All electrochemical experiments were performed in a home-made three-electrode cell with a PAR Potentiostat/Galvanostat model 283 (Princeton Applied research) at room temperature. The working electrodes were prepared by depositing a nanoparticle suspension onto clean indium–tin oxide (ITO) coated glass slices (size: $20 \times 20\ mm^2$, resistance: $\leqslant 20\ \Omega$ (=sheet resistance $20\ \Omega$/sq), Präzisions Glas & Optik GmbH, Iserlohn, Germany) and dried in Ar flow. The size of the deposited spot was measured, and the current density was calculated by using the apparent size of each electrode. A Ag/AgCl electrode (Metrohm AG) in 3 M KCl was used as the reference electrode and a pure gold plate as the counter electrode. The electrolyte for electrochemical reaction was deaerated by bubbling with Ar for 20 min before each measurement.

3. Results and discussion

The field emission scanning electron microscope (FE-SEM) images in Fig. 1 indicated the morphological features of the samples. The {1 1 0} Au nanobelts have an average thickness and width of 30 nm and 250–300 nm, respectively. The average length is about 20 μm (Fig. 1a). The {1 1 0} Au nanoplates show a square shape with a side length of 70–100 nm and thickness of 20 nm (Fig. 1b). Chemically synthesized {1 1 1} Au nanoplates have a hexagonal shape, with a size of 1–1.5 μm and thickness of 50 nm (Fig. 1c). Various techniques confirmed that Au nanobelts and square-shaped nanoplates are enclosed by {1 1 0} surface, while hexagonal Au nanoplates are surrounded solely by {1 1 1} facets. The details of the morphological and structural analysis can be found in Refs. [15–20].

Previous studies have shown that the glucose oxidation on gold strongly depends on the crystallographic orientation of the electrode [21,22]. For the three basal planes of gold, they displayed different electrocatalytic activities under different conditions [21,22]. In this work, glucose oxidation was investigated in either alkaline or neutral media. Fig. 2a shows the typical voltammetric curves at Au {1 1 0} nanobelts, {1 1 0} nanoplates and {1 1 1} nanoplates in 0.1 M NaOH solution containing 10 mM glucose. A step-wise oxidation appears to be involved in the reaction for Au nanobelts and nanoplates with {1 1 0} surface. Two interesting large oxidation peaks were observed at ca. −0.24 V (vs. SHE, in the following all potentials refer to SHE) and 0.3–0.5 V (broad peak), which correspond to the oxidation of glucose and further oxidation of gluconolactone generated by the first oxidation peak, respectively [21–23]. For {1 1 1} nanoplates, the oxidation peak is at 0.46–0.52 V, this is in accordance with the second oxidation peak for the other two samples. However, the first oxidation peak at −0.24 V was absent. The onset of glucose oxidation for {1 1 1} nanoplates is at about 0.2 V, this is more than 500 mV positively shifted compared with the other two samples. Similar results were found for glucose in neutral solution, as shown in Fig. 2b. The onset of glucose oxidation on {1 1 1} nanoplates is at 0.32 V, it is about 400 mV positively shifted compared to samples with {1 1 0} surface. For {1 1 0} nanobelts and nanoplates, one major oxidation peak and a post peak were found at ca. 0.24–0.29 V and 0.57 V, respectively, while the main oxidation peak for {1 1 1} nanoplates was located at 0.56 V. A comparison of the CVs in Fig. 2b indicated that the main oxidation peak for {1 1 1} nanoplates coincides with the post peak for the other two samples. This means that the oxidation of glucose at 0.24–0.29 V (the main oxidation peak for {1 1 0} samples) was suppressed for {1 1 1} nanoplates. So, one can see that the electrocatalytic activity of {1 1 0} nanobelts and

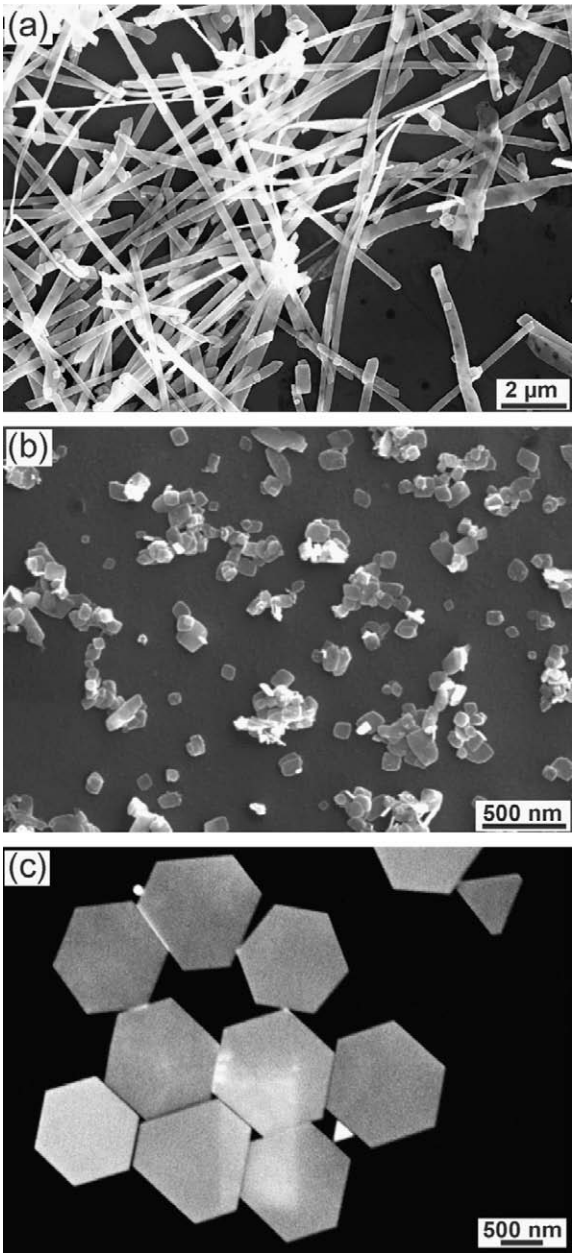

Fig. 1. FE-SEM images of (a) Au nanobelts, (b) {1 1 0} Au nanoplates with a square shape and (c) {1 1 1} Au nanoplates with hexagonal shape.

nanoplates is much higher than that of {1 1 1} nanoplates in both, alkaline and neutral media. The largely enhanced catalytic activity of the {1 1 0} Au nanobelts and nanoplates may be attributed to the higher density of stepped atoms on gold {1 1 0} plane.

In order to find out whether or not the {1 1 0} surface of gold always leads to a higher electrocatalytic performance as compared to the {1 1 1} plane, methanol oxidation was used as a further probe reaction. Fig. 2c shows a comparison of cyclic voltammograms (CVs) in 0.1 M NaOH solution containing 1.5 M methanol for the three samples. To preserve the superficial structure of the samples, the oxidation of the surface has been avoided by setting the upper potential limit below 0.8 V [19,24]. A strong and broad oxidation peak was found at 0.37–0.50 V for the {1 1 1} nanoplates, which can be ascribed to the oxidation of methanol to formates as the final product through a four-electron transfer reaction [19,24,25]. The oxidation peak is very broad, so it may be composed of two

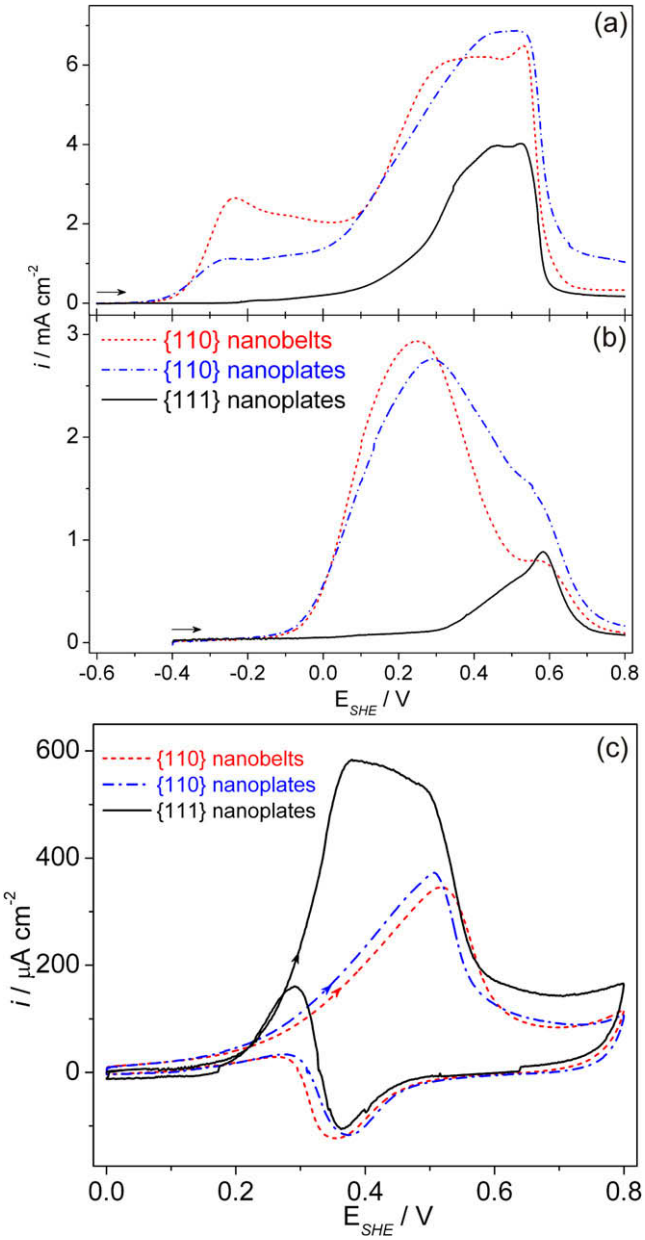

Fig. 2. Typical voltammetric curves of {1 1 0} Au nanobelts, {1 1 0} nanoplates and {1 1 1} nanoplates in (a) 0.1 M NaOH with 10 mM glucose, (b) phosphate buffer (pH = 7.4) with 10 mM glucose, and (c) 0.1 M NaOH with 1.5 M CH_3OH, respectively. Scan rate: 20 mV/s.

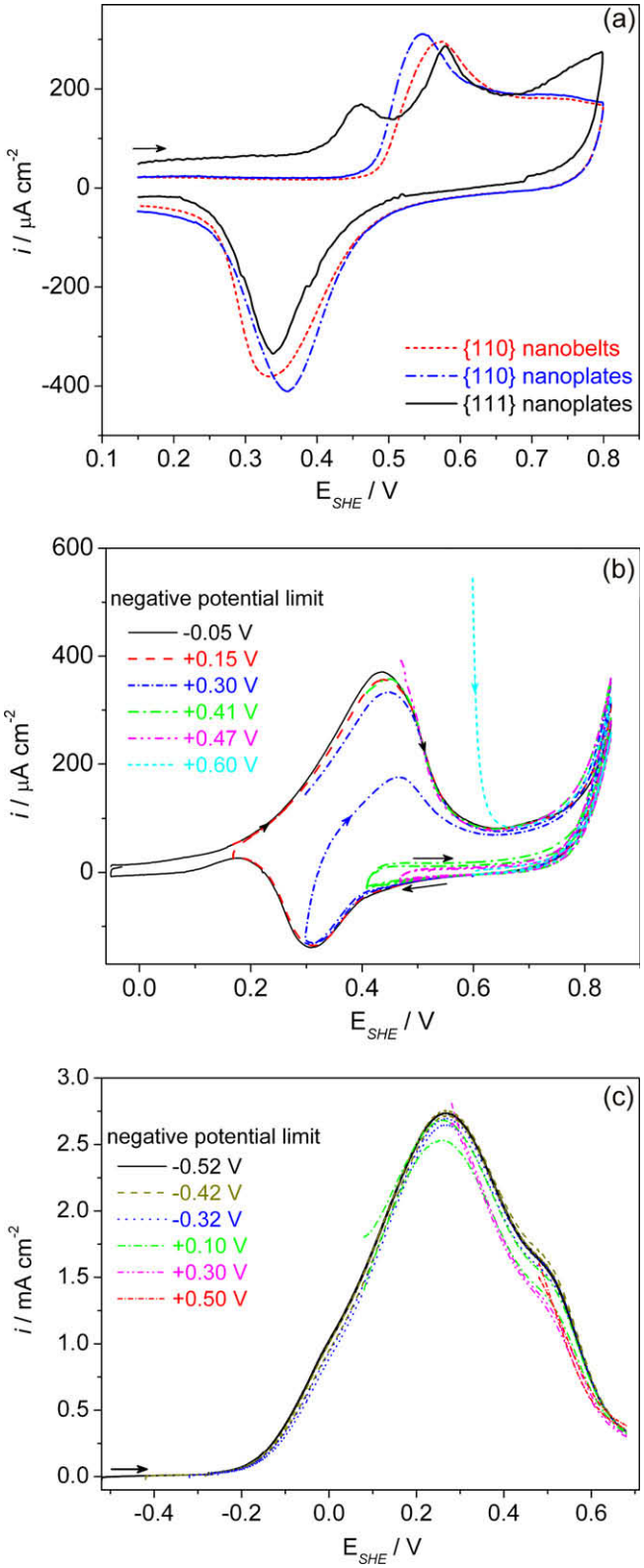

Fig. 3. (a) Cyclic voltammograms of {1 1 0} Au nanobelts, {1 1 0} nanoplates and {1 1 1} nanoplates in 0.1 M NaOH solution without the presence of CH_3OH. (b) Cyclic voltammograms of {1 1 0} Au nanobelts in 0.1 M NaOH with 1.5 M CH_3OH, (c) positive scan of cyclic voltammograms of {1 1 0} Au nanobelts in phosphate buffer (pH = 7.4) with 10 mM glucose with different negative potential limits. Scan rate: 20 mV/s.

closely located peaks. Indeed, for methanol oxidation on a Au {1 1 1} macro-electrode, there is a pre-peak representing methanol oxidation only and a main peak representing the sum of methanol oxidation and gold oxide formation [24]. The difference is that in Ref. [24], the first peak is rather weak compared with the present case, and this may be because of low electrocatalytic properties of the used macro-electrode in that case. By comparing CVs from different samples, surprisingly, it was found that the oxidation peaks for {1 1 0} nanobelts and nanoplates showed a significant positive shift of 120–150 mV compared with the {1 1 1} nanoplates. The oxidation peaks for {1 1 0} Au nanobelts and nanoplates started from 0.25 V, increased slowly and reached the maximum only at 0.50–0.52 V. Compared with {1 1 1} Au nanoplates, this is much positively shifted, and the peak potential is accordant with the post peak for {1 1 1} Au nanoplates. One possible explanation for this behavior is a primary adsorption so that the adsorbed species are quickly oxidized during the scan but a current decay is observed since the absorbed species are consumed. This will be

investigated in a follow up work by means of potential step experiments and scan rate dependent voltammetry. In the cease of methanol oxidation the rate occurs at almost the same potential for all samples (0.55 V). Moreover, the current density of the oxidation peak on {1 1 1} Au nanoplates is about two times higher. Even for the negative scan, the oxidation peak at 0.3 V on the reactivated {1 1 1} Au nanoplates is higher than for the other two samples. In this case, the {1 1 1} surface of gold shows obviously a higher electrocatalytic ability towards methanol oxidation than the {1 1 0} surface.

To explore the reason for this 'unusual' phenomenon, the voltammetric behavior of these samples in the supporting solution (0.1 M NaOH) was studied. As shown in Fig. 3a, characteristic oxidation and reduction peaks are observed for all three kinds of samples. For {1 1 0} Au nanobelts and nanoplates, one major oxidation peak at ca. 0.55 V was observed representing the formation of surface oxides [26,27]. However, a strong peak at 0.46 V appeared before the onset of surface oxidation for {1 1 1} nanoplates. The first oxidation peak on Au {1 1 1} surface corresponds to the potential-induced anion (OH^-) adsorption and the partial discharge of OH^- anions [26,27]. According to Borkowska et al. [24], not only adsorbed OH^- anions, but also partially discharged OH species are needed for methanol oxidation, which is different in the case of glucose oxidation. Apparently, this process occurs at more negative potentials on {1 1 1} nanoplates than on the other two samples, thus the induction of methanol oxidation starts at the most negative potential.

The potential-range dependence for methanol and glucose oxidation was examined by increasing the negative potential limits gradually. When the negative potential limit increases, the absorption of OH^- will be hindered for the second cycle during two successive CV sweeps. As seen from Fig. 3b, for methanol oxidation, the oxidation peak current of the second cycle started to decrease when the negative potential limit reached 0.3 V. At a potential negative of 0.4 V, the oxidation of methanol for the second cycle was hindered almost completely. When the negative potential limit was not low enough to reduce the surface oxide, the adsorption of OH^- specie and its successive discharge could not occur during the positive sweep of the second cycle. It is, therefore, a reasonable assumption that the adsorbed OH^- and partially discharged OH^- species are of crucial importance for the oxidation of methanol. For glucose oxidation on the other hand, the oxidation peaks of the second scan remained nearly the same as the first one when rising the negative potential limit, as seen from Fig. 3c. This indicates that the adsorption of OH^- is not a key factor in starting glucose oxidation. Indeed, according to Adzic et al. [21], glucose oxidation can start on gold surface without a strong adsorption of OH^-. Thus, the nature of the electrode seems to be the crucial factor for glucose oxidation. The higher electrocatalytic ability of Au {1 1 0} facets towards glucose oxidation may result from the higher surface energy compared with {1 1 1} surface, this is different from that of the methanol oxidation.

4. Conclusions

In summary, gold nanobelts and nanoplates enclosed by different crystallographic surfaces, {1 1 0} or {1 1 1} surface, have different electrochemical properties. Surprisingly, the {1 1 0} surface of gold does not always show a higher electrocatalytic activity than the {1 1 1} surface. This is due to the different mechanisms of the electrochemical reactions. These nanobelts and nanoplates provide the ideal class of materials for the investigation of other possible anisotropic properties.

Acknowledgments

Y. Chen acknowledges International Max-Planck Research School (IMPRS) – SurMat for financial support through a Doctoral fellowship. The financial support of the Deutsche Forschungsgemeinschaft within the DFG Priority Program 1165 "Nanowires and Nanotubes – from Controlled Synthesis to Function" (HA 3118/4-3) is gratefully acknowledged. We are indebted to Dr. S. Milenkovic for the metallurgical processing of the pre-alloys.

References

[1] N. Tian, Z.Y. Zhou, S.G. Sun, Y. Ding, Z.L. Wang, Science 316 (2007) 732.
[2] N. Tian, Z.Y. Zhou, S.G. Sun, J. Phys. Chem. C 112 (2008) 19801.
[3] S.G. Sun, A.C. Chen, T.S. Huang, J.B. Li, Z.W. Tian, J. Electroanal. Chem. 340 (1992) 213.
[4] G.A. Somorjai, D.W. Blakely, Nature 258 (1975) 580.
[5] H.G. Liao, Y.X. Jiang, Z.Y. Zhou, S.P. Chen, S.G. Sun, Angew. Chem., Int. Ed. 47 (2008) 9100.
[6] A.R. Tao, S. Habas, P. Yang, Small 4 (2008) 310.
[7] M. Subhramannia, V.K. Pillai, J. Mater. Chem. 18 (2008) 5858.
[8] B.K. Jena, C.R. Raj, Electrochem. Commun. 10 (2008) 951.
[9] P. Rodriguez, E. Herrero, J. Solla-Gullon, J.M. Feliu, A. Aldaz, J. Solid State Electrochem. 12 (2008) 575.
[10] J. Solla-Gullon, F.J. Vidal-Iglesias, A. Lopez-Cudero, E. Garnier, J.M. Feliu, A. Aldaza, Phys. Chem. Chem. Phys. 10 (2008) 3689.
[11] F.J. Vidal-Iglesias, J. Solla-Gullon, P. Rodriguez, E. Herrero, V. Montiel, J.M. Feliu, A. Aldaz, Electrochem. Commun. 6 (2004) 1080.
[12] J. Hernandez, J. Solla-Gullon, E. Herrero, A. Aldaz, J.M. Feliu, J. Phys. Chem. C 111 (2007) 14078.
[13] Z.L. Wang, J. Phys. Chem. B 104 (2000) 1153.
[14] R. Chetty, S. Kundu, W. Xia, M. Bron, W. Schuhmann, V. Chirila, W. Brandl, T. Reinecke, M. Muhler, Electrochim. Acta 54 (2009) 4208.
[15] A.W. Hassel, M. Seo, Electrochim. Acta 44 (1999) 3769–3777.
[16] S. Milenkovic, A. Schneider, A.W. Hassel, Gold Bull. 39 (2006) 185.
[17] Y. Chen, S. Milenkovic, A.W. Hassel, Nano Lett. 8 (2008) 737.
[18] Y. Chen, C. Somsen, S. Milenkovic, A.W. Hassel, J. Mater. Chem. 19 (2009) 924.
[19] Y. Chen, S. Milenkovic, A.W. Hassel, submitted for publication.
[20] Y. Chen, X. Gu, C.G. Nie, Z.Y. Jiang, Z.X. Xie, C.J. Lin, Chem. Commun. (2005) 4181.
[21] R.R. Adzic, M.W. Hsiao, E.B. Yeager, J. Electroanal. Chem. 260 (1989) 475.
[22] M.W. Hsiao, R.R. Adzic, E.B. Yeager, J. Electrochem. Soc. 143 (1996) 759.
[23] M. Tominaga, T. Shimazoe, M. Nagashima, I. Taniguchi, Electrochem. Commun. 7 (2005) 189.
[24] Z. Borkowska, A. Tymosiak-Zielinska, G. Shul, Electrochim. Acta 49 (2004) 1209.
[25] N. Zhao, Y. Wei, N.J. Sun, Q.J. Chen, J.W. Bai, L.P. Zhou, Y. Qin, M.X. Li, L.M. Qi, Langmuir 24 (2008) 991.
[26] A. Hamelin, M.J. Sottomayor, F. Silva, S.C. Chang, M.J. Weaver, J. Electroanal. Chem. 295 (1990) 291.
[27] J. Hernandez, J. Solla-Gullon, J. Hernandez, A. Aldaz, J.M. Feliu, Electrochim. Acta 52 (2006) 1662.